

Supporting Information (SI)

Controlled aggregation of the core(amorphous silica)@shell(TPA-polysilicates) nanoparticles at room temperature by selective removal of TPA⁺ ions from nanoparticle shell

Sanja Bosnar,^a Maja Dutour Sikirić,^b Vilko Smrečki,^c Josip Bronić,^a Suzana Šegota,^b Vida Strasser,^b Tatjana Antonić Jelić,^a Ana Palčić,^a and Boris Subotić ^{*a}

^a*Laboratory for Synthesis of New Materials, Division of Materials Chemistry, Ruder Bošković Institute, Bijenička 54, 10000 Zagreb, Croatia. E-mail: sbosnar@irb.hr; bronic@irb.hr; tantonic@irb.hr; Ana.Palcic@irb.hr; subotic@irb.hr*

^b*Laboratory for Biocolloids and Surface Chemistry, Division of Physical Chemistry, Ruder Bošković Institute, Bijenička 54, 10 000 Zagreb, Croatia. E-mail: sikiric@irb.hr; ssegota@irb.hr; Vida.Strasser@irb.hr*

^c*NMR Center, Ruder Bošković Institute, Bijenička 54, 10000 Zagreb, Croatia. E-mail: smrecki@irb.hr*

The content of listed materials

SI-1: Hydrolysis of tetraethyl orthosilicate (TEOS) in alkaline solutions, the formation of silica nanoparticles and results of pH measurements

SI-2: Presentation and explanation of additional DLS-PSD data

SI-3: Simplification of schematic presentation of nanoparticle shell

SI-4: ²⁹Si-NMR analysis

Additional references

SI-1: Hydrolysis of tetraethyl orthosilicate (TEOS) in alkaline solutions, the formation of silica nanoparticles and results of pH measurements

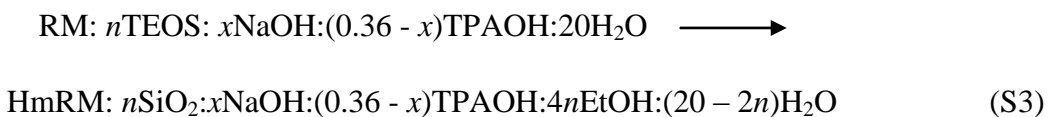
Formally, hydrolysis of TEOS $[\text{Si}(\text{OC}_2\text{H}_5)_4]$ in alkaline solution, results in the formation of SiO_2 and ethanol ($\text{C}_2\text{H}_5\text{OH}$ - EtOH),^{A1,A2} i.e.,



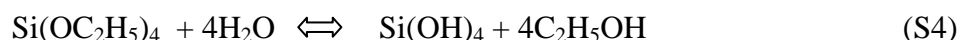
Hence, the hydrolysis of TEOS, in alkaline water solution, results in the formation of the homogeneous reaction mixture HmRM (clear solution), containing water, EtOH, base (ROH) and SiO_2 in the form of silica nanoparticles and different soluble silicate species (monomers and oligomers),^{21,34,35,48,49,50} i.e.,



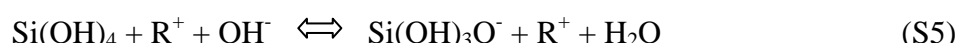
or in our case



where $n = 0.2$ and 1 , $a\text{ROH} = 0.36\text{ROH} = x\text{NaOH} + (0.36 - x)\text{TPAOH}$ and $0 \leq x \leq 0.054$ (see Experimental in the main text). However, in reality, early stage of the hydrolysis of TEOS in the presence of strong inorganic (NaOH, KOH, RbOH, CsOH, etc.) and/or organic (tetraalkylammonium hydroxides - TAAOH) bases does not result in the direct formation of silica (SiO_2), but in silicate monomers,^{34,35,47,48,52} i.e.,



which then are deprotonated by the reaction with the OH^- ions from solution, i.e.,



and thus,



Mutual reactions of such formed deprotonated monomers lead to the formation of different soluble (poly)silicate anions (small oligomers).^{21,34,47-49,52} Since it was found that the reactions between single-charged and neutral silicate species are favoured over those involving either two neutral or two charged species,⁶⁷ it is reasonable to assume that a part of the $\text{Si}(\text{OH})_4$ monomers could be involved in the formation of small silicate oligomers, before deprotonation. The processes of the formation of the $\text{Si}(\text{OH})_4$ monomers [Eq. (S4)], their deprotonation [Eq. (S5)] and formation of small silicate oligomers take place below the critical aggregation concentration (CAC), i.e., when the value $[\text{OH}^-]_{\text{tot}}/[\text{SiO}_2]_{\text{tot}} \geq 1$.^{21,34,35,48-50,52} Here, $[\text{OH}^-]_{\text{tot}}$ is the total amount (expressed as the molality concentration or mole fraction) of the OH^- ions in the HmRM and $[\text{SiO}_2]_{\text{tot}}$ is the amount (expressed as the molality concentration or mole fraction) of the SiO_2 (in the form of silicate monomers, oligomers and nanoparticles) formed by the complete hydrolysis of TEOS. There is a widely spread opinion that for $[\text{OH}^-]_{\text{tot}}/[\text{SiO}_2]_{\text{tot}} > 1$, i.e., below the CAC, only silicate monomers and small oligomers, but not silica nanoparticles exist in the HmRM.^{21,34,35,47-49,52} This is argued by the fact that, below the CAC, the silica nanoparticles cannot be detected by ²⁹Si-NMR^{14,16,21,34,49,57,A3} or by the small-angle X-ray scattering (SAXS).^{14,34,35,47,48,50,65,A3} On the other hand, using the same techniques (²⁹Si-NMR, SAXS), the formation of the silica nanoparticles, often called the primary nanoparticles (PNPs) or the primary precursor species (PPSs), is observed when $[\text{OH}^-]_{\text{tot}}/[\text{SiO}_2]_{\text{tot}}$ is 1 or lower,^{14,16,21,43,35,47-50,57,65} (above the CAC), i.e., when the concentration of OH^- ions is not sufficient for deprotonation of the $\text{Si}(\text{OH})_4$ monomers formed by hydrolysis of TEOS. In the other words, when a critical concentration of the $\text{Si}(\text{OH})_4$ monomers is reached, self-assembly starts leading to a stable suspension of aggregated monomer particles (PNPs).⁴⁸ However, in spite of the widely spread opinion that the silica nanoparticles cannot be formed below the CAC,^{15,16,21,27,34,35,47-51,65} the resolutely evidence of the formation of the stable, ≈ 1.2 nm-sized core(amorphous SiO_2)@shell(TPA^+ ions) nanoparticles below the CAC was found by dynamic light scattering (DLS) and atomic force microscopy (AFM).⁵² This is also confirmed in this work: Although the nanoparticles cannot be identified in the ²⁹Si-NMR spectrum of HmRM_{0-II} (see Fig. 5A and Experimental in the main text), the DLS-PSD curve in Fig. 6A and AFM images in Figs. 7A and 7A' in the main text, clearly show that the primary silica nanoparticles (PNPs) are formed below the

CAC ($[\text{OH}^-]_{\text{tot}}/[\text{SiO}_2]_{\text{tot}} = 1.8 > 1$) in the $\text{HmRM}_0\text{-II}$. The subsequent addition of NaOH causes aggregation and coalescence of the PNPs, formed in the absence of NaOH (see Figs. 6B, 7B and 7B' in the main text). On the other hand, in the HmRMs , formed above the CAC ($[\text{OH}^-]_{\text{tot}}/[\text{SiO}_2]_{\text{tot}} = 0.36 < 1$), the silica nanoparticles are formed (see Figs. 1 and 2 in the main text) for each value of x , regardless of the mode (subsequent: $x = x_s$ or direct: $x = x_d$) of the NaOH addition (see Experimental in the main text).

In accordance with Eqs. (S5) and (S6), deprotonation of the silicate monomers, formed by the hydrolysis of TEOS, causes a drop of the concentration of OH^- ions from $[\text{OH}^-] = [\text{OH}^-]_{x,0}$ at $t_s = 0$ to $[\text{OH}^-] = [\text{OH}^-]_{x,t}$ at any time $t_s > 0$. In accordance with the previously established procedure,⁵² the molality concentrations, $[\text{OH}^-]_{\text{calc},x,0} = [\text{TPAOH}]_{\text{calc},x,0} + [\text{NaOH}]_{\text{calc},x,0}$ were calculated from the corresponding chemical compositions of the TEOS-free reaction mixtures,

RM1: $x\text{NaOH}:(0.36 - x)\text{TPAOH}:20\text{H}_2\text{O}$ and

RM2: $x\text{NaOH}:(0.36 - x)\text{TPAOH}:4\text{EtOH}:18\text{H}_2\text{O}$

Comparison of the pH values, calculated as: $\text{pH}(\text{calc})_{x,0} = 14 + \log\{[\text{OH}^-]_{\text{calc},x,0}\}$ and the values, $\text{pH}(\text{meas1})_{x,0}$, measured in RM1, has shown that their difference $(\Delta\text{pH})_x = \text{pH}(\text{calc})_{x,0} - \text{pH}(\text{meas1})_{x,0}$ slightly decreases from 0.051 for $x = x_s = x_d = 0$ to 0.037 for $x = x_d = 0.054$. This is consistent with the results of previous analyses,⁵² showing a slight increase of the ion-pair association with decreasing value of x and thus, with the increasing concentration of TPAOH in the investigated reaction mixtures. As expected from the previous study,⁵² the values $\text{pH}(\text{meas1})_{x,0}$ and $\text{pH}(\text{meas2})_{x,0}$, measured in RM1 and RM2, respectively, are almost the same, thus showing that the ethanol, formed during the hydrolysis of TEOS (see Eq. S6), does not affect the measured pH [$\text{pH}(\text{meas1})_{x,0} \approx \text{pH}(\text{meas2})_{x,0}$] in the investigated reaction mixtures. Hence,

$$(\text{pH})_{x,0} = \text{pH}(\text{meas})_{x,0} + (\Delta\text{pH})_x \quad (\text{S7})$$

where, $\text{pH}(\text{meas})_{x,0} = [\text{pH}(\text{meas1})_{x,0} + \text{pH}(\text{meas2})_{x,0}]/2$. By the same principle,

$$(\text{pH})_{x,24h} = \text{pH}(\text{meas})_{x,24} + (\Delta\text{pH})_x \quad (\text{S8})$$

where, $\text{pH(meas)}_{x,24}$ are the measured values of pH in the HmRMs aged for $t_A = 24$ h and/or $t_A' = 24$ h (see Experimental in the main text). The characteristic molality concentrations $[\text{OH}^-]_{x,0}$, $[\text{OH}^-]_{x,24h}$ and the corresponding pH values, $(\text{pH})_{x,0}$ and $(\text{pH})_{x,24h}$ are listed in the Table S1 as functions of x (x_s , x_d) and R (R_s and R_d), where $R = x/0.36$.

Table S1 The values $(\text{pH})_{x,0}$, calculated by Eq. (S7) and $(\text{pH})_{x,24h}$, calculated by Eq. (S8), as well as the corresponding concentrations of OH^- ions, calculated as: $[\text{OH}]_{x,0} = 10^{[14 - (\text{pH})_{x,0}]}$ and $[\text{OH}]_{x,24h} = 10^{[14 - (\text{pH})_{x,24h}]}$, presented as functions of x (x_s , x_d) and R (R_s , R_d). Meanings of the measured values $\text{pH(meas1)}_{x,0}$, $\text{pH(meas2)}_{x,0}$ and $\text{pH(meas)}_{x,24}$ are described in the text above.

x	R	$(\text{pH})_{x,0}$	$[\text{OH}^-]_{x,0}$ (mol/kg)	$(\text{pH})_{x,24h}$	$[\text{OH}^-]_{x,24h}$ (mol/kg)
$x_s = x_d = 0$	$R_s = R_d = 0$	13.805	0.6386	12.853	0.0713
$x_s = 0.0018$	$R_s = 0.005$	13.805	0.6389	12.840	0.0692
$x_s = 0.0036$	$R_s = 0.010$	13.806	0.6393	12.837	0.0687
$x_s = 0.0108$	$R_s = 0.030$	13.807	0.6406	12.849	0.0706
$x_s = 0.0144$	$R_s = 0.040$	13.807	0.6413	12.830	0.0676
$x_s = 0.0180$	$R_s = 0.050$	13.807	0.6419	12.867	0.0736
$x_d = 0.0180$	$R_d = 0.050$	13.807	0.6419	12.845	0.0702
$x_d = 0.0270$	$R_d = 0.075$	13.809	0.6436	12.871	0.0743
$x_d = 0.0360$	$R_d = 0.100$	13.810	0.6453	12.786	0.0611
$x_d = 0.0396$	$R_d = 0.110$	13.810	0.6460	12.830	0.0676
$x_d = 0.0468$	$R_d = 0.130$	13.811	0.6474	12.827	0.0671
$x_d = 0.0540$	$R_d = 0.150$	13.812	0.6487	12.813	0.0650

The results presented in the Table S1 show that both the starting $[(\text{pH})_{x,0}, [\text{OH}^-]_{x,0}]$ and the “ending” $[(\text{pH})_{x,24h}, [\text{OH}^-]_{x,24h}]$ pH values and the concentrations of the “free” OH^- ions do not depend on the fraction of the TPAOH substituted by NaOH, added in the reaction mixtures either subsequently ($x = x_s$, $R = R_s$) or directly ($x = x_d$, $R = R_d$) (see Experimental in the main text). Since, from one side, the total amount of the OH^- ions is constant, i.e., $x\text{NaOH}:(0.36 - x)\text{TPAOH} = 0.36$ and from the other side, both TPAOH and NaOH are strong, entirely dissociated bases, the independence of $(\text{pH})_{x,0}$, $[\text{OH}^-]_{x,0}$, $(\text{pH})_{x,24h}$ and $[\text{OH}^-]_{x,24h}$, are expected. $(\text{pH})_{x,24h}$, represents the value of pH, determined by the pseudo-equilibrium

concentration, $[\text{OH}^-]_{x,24\text{h}}$, of the “free” OH^- ions present in the investigated HmRMs at $t_{\text{A}'} = 24$ h for subsequently added NaOH , and $t_{\text{A}} = 24$ h for directly added NaOH , respectively. The difference, $[\text{OH}^-]_{x,0} - [\text{OH}^-]_{x,24\text{h}}$ represent the amount (expressed as molality concentrations) of the OH^- ions spent for deprotonation of $\text{Si}(\text{OH})_4$ monomers [see Eqs (S5) and (S6)] during the early stage of hydrolysis as well as for deprotonation of the terminal $\equiv\text{Si}–\text{OH}$ groups of oligomers and nanoparticles during the *rt* ageing.⁵²

SI-2: Presentation and explanation of additional DLS-PSD data

Stirring of the Na^+ -free RM: TEOS:0.36TPAOH:20H₂O (RM₀-I) at room temperature (*rt*) and its additional *rt* ageing under static conditions for $t_A = 24$ h (see Experimental in the main text) results in the formation of the core(amorphous silica)@shell(TPA-polysilicates) nanoparticles (primary nanoparticles - PNPs; see Schemes 1A, 1B and 1C₁ in the main text) in the corresponding homogeneous reaction mixture (HmRM₀-I: SiO₂:0.36TPAOH:4EtOH:18H₂O) (solid curve in Fig. S1A; see also Fig. 1A in the main text). The formed nanoparticles have the sizes in the range from $D_{\min}(N) \approx 1$ nm to $D_{\max}(N) = 3.6$ nm with $D_p(N) = 1.74$ nm. The „particles“ having the sizes in the range from about 0.46 to about 0.96 nm (in the DLS-PSDs by number and volume in Fig. S1A) possibly correspond to the polysilicate anions (oligomers) associated with TPA⁺ ions or even the core@shell particles at the early stage of formation.⁵¹

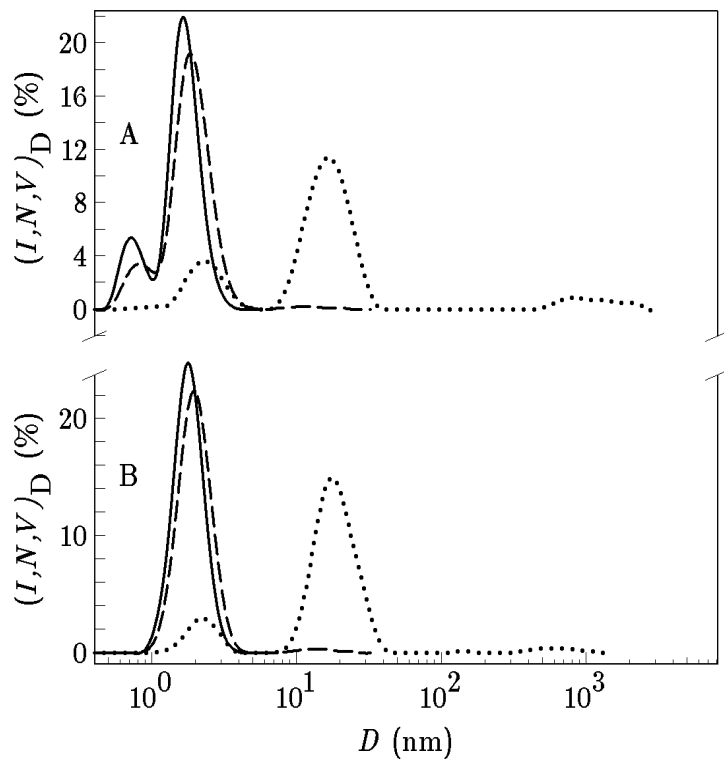


Fig. S1 DLS-PSDs by number (solid curves), volume (dashed curves) and intensity (dotted curves) of the NaOH-free HmRM₀-I (see Experimental in the main text), stirred at room temperature (*rt*) for $t_s = 120$ min and then, additionally aged at *rt*, under static conditions, for (A): $t_a = 22$ h ($t_A = t_s + t_a = 24$ h) and (B): $t_a = 37$ d ($t_A \approx 37$ d). N_D is the number percentage, V_D is the volume (mass) percentage and I_D is the scattering intensity percentage of the particles having the spherical equivalent diameter D .

The multi-modal PSDs by intensity are consistent with the already published data.^{14,19,26,33,56,A4} However, from the relationship between the particle size and the intensity of scattered light^{51,56,A5} it can be easily calculated that the particles with $D_p(I) = 15.69$ nm [dotted curves in Fig. S1; $D_p(I)$ is the diameter at the „peak“ intensity] represent about 0.002 % of the total number of particles; the percentage of the particles with $D_p(I) = 955$ nm is negligible. This is the reason that the population of the larger particles cannot be detected in the DLS-PSDs by number and volume. However, the presence of a fraction of larger particles ($D_p(I) = 15.69$ nm) in the PSD by intensity, points out to the mutual aggregation of a very small fraction of the PNPs.²⁹ By the same principle, it can be assumed that the extremely small fraction of the largest particles ($D_p(I) = 955$ nm) is formed by mutual aggregations of the PNPs and the larger particles ($D_p(I) = 15.69$ nm). The particles size distributions (by number, volume and intensity), established at $t_A = 24$ h do not (considerably) change during the prolonged room temperature ageing of the HmRM₀-I at least to $t_A = 37$ d (Fig. S1B). The reasons for the high stability of the PNPs, formed in HmRM₀-I, are explained in the main text.

As already is stated and explained in the main text, the addition of very small amount ($x_s = 0.0018$, $R_s = x_s/0.36 = 0.005$) of sodium hydroxide to the 1a-HmRMs (1a-HmRMs -> 1aS-HmRMs; see Experimental in the main text), immediately causes intensive aggregation processes. The consequence is that at $t_s \leq 40$ min (t_s is the time passed after the addition of NaOH into NaOH-free HmRM; see Experimental in the main text), at least six particle populations are present in the system (see Fig. S2A). Four of them, characterized by $D_p(N)_1 = D_p(V)_1 = D_p(I)_1 = 1.117$ nm, $D_p(N)_2 = D_p(V)_2 = D_p(I)_2 = 2.696$ nm, $D_p(N)_3 = D_p(V)_3 = D_p(I)_3 = 4.894$ nm and $D_p(N)_4 = D_p(V)_4 = D_p(I)_4 = 8.721$ nm are detected in the DLS-PSDs by number, volume and intensity, respectively. It is evident that the aggregation processes, but with smaller intensity, take place for $t_s > 40$ min and that the particle population (by number and volume) having the size of about 7.5 nm is the dominant one (90 % by number) at $t_A = 24$ h (Fig. S2B; see also Fig. 1B in the main text). The size of the dominant particle populations (by number and volume) increases from $D_p(N) = D_p(V) = 7.5$ nm at $t_A = 24$ h (Fig. S2B) to $D_p(N) \approx D_p(V) \approx 13.6$ nm at $t_A = 8$ d (Fig. S2C). However, it is interesting that the particle population, characteristic for the PNPs [$D_p(N) = D_p(V) = 1.736$ nm; Fig. S1] again appears at $t_A = 8$ d (Fig. S2C). Taking into consideration that the larger particles represent aggregates of the PNPs (see Fig. 1E, 1E' and 2 and the corresponding discussion in the main text), this indicates that a part of the larger particles (aggregates) disaggregate into the starting PNPs in

the time interval from $t_{A'} \geq 24$ h to $t_{A'} \leq 8$ d; the reason is discussed and explained in the main text as well as later, in this section.

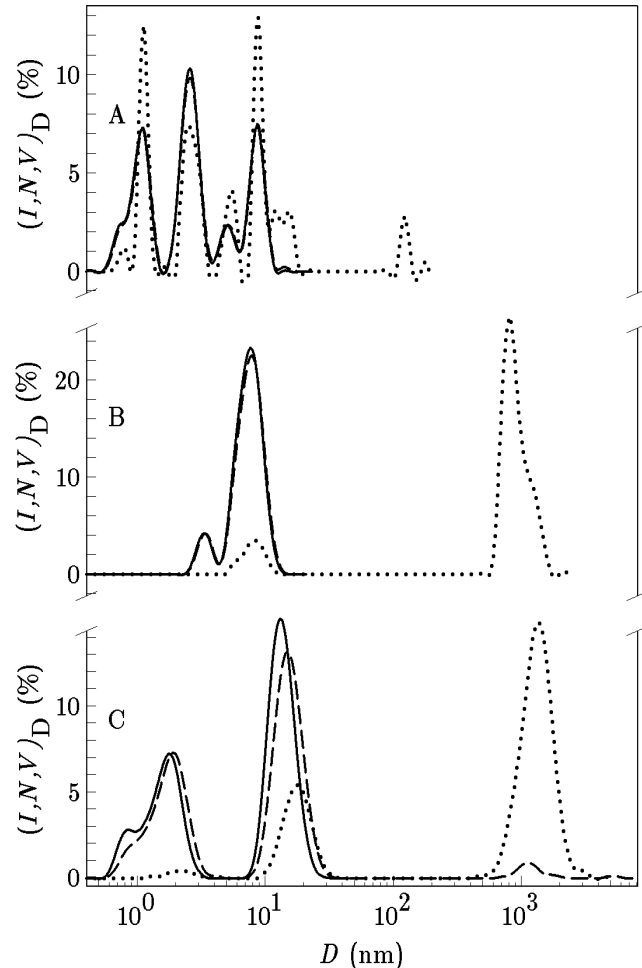


Fig. S2 DLS-PSDs by number (solid curves), volume (dashed curves) and intensity (dotted curves) of the 1aS-HmRM, characterized by $x_s = 0.0018$, and $R_s = x_s/0.36 = 0.005$, stirred/aged at room temperature for $t_{s'} = 40$ min (A), $t_{A'} = 24$ h (B) and $t_{A'} = 8$ d (C), after the addition of NaOH into the NaOH-free 1a-HmRM. $t_{s'}$ is the time of *rt* stirring passed after the addition of NaOH into NaOH-free HmRM and $t_{A'} = t_{s'} + t_a$, where t_a is the time of additional *rt* aging under static conditions (see Experimental in the main text). N_D is the number percentage, V_D is the volume (mass) percentage and I_D is the scattering intensity percentage of the particles having the spherical equivalent diameter D .

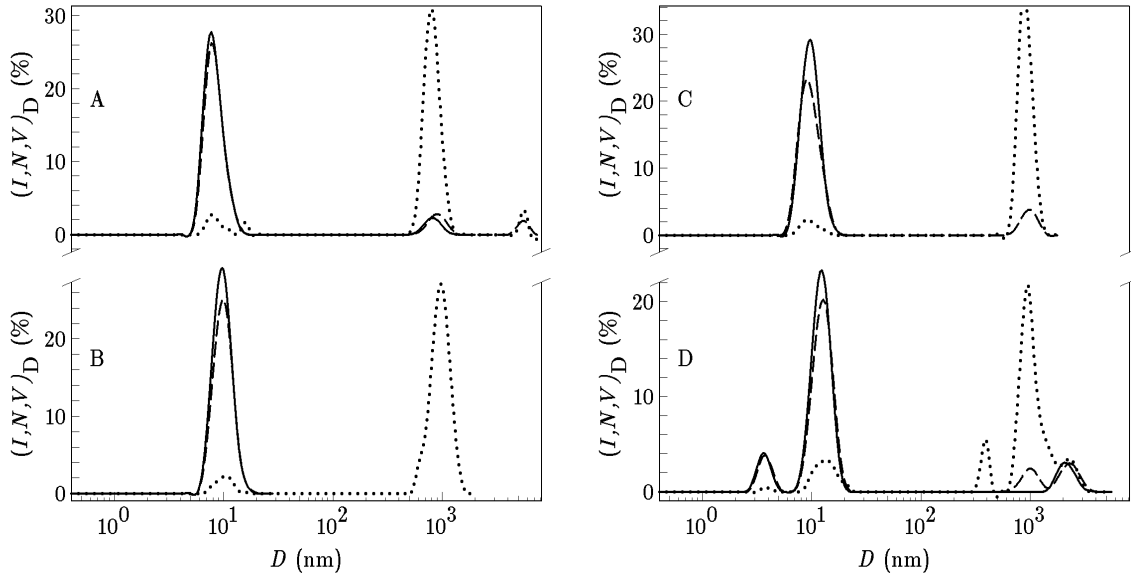


Fig. S3 DLS-PSDs by number (solid curves), volume (dashed curves) and intensity (dotted curves) of the 1aS-HmRM, characterized by $x_s = 0.0036$ and $R_S = x_s/0.36 = 0.01$, stirred/aged at room temperature for $t_s' = 40$ min (A), $t_s' = 80$ min (B), $t_s' = 120$ min (C) and $t_{A'} = 24$ h (D), after the addition of NaOH into the NaOH-free 1a-HmRM. t_s' is the time of *rt* stirring passed after the addition of NaOH into NaOH-free 1a-HmRM and $t_{A'} = t_s' + t_a'$, where t_a' is the time of additional *rt* aging under static conditions (see Experimental in the main text). N_D is the number percentage, V_D is the volume (mass) percentage and I_D is the scattering intensity percentage of the particles having the spherical equivalent diameter D .

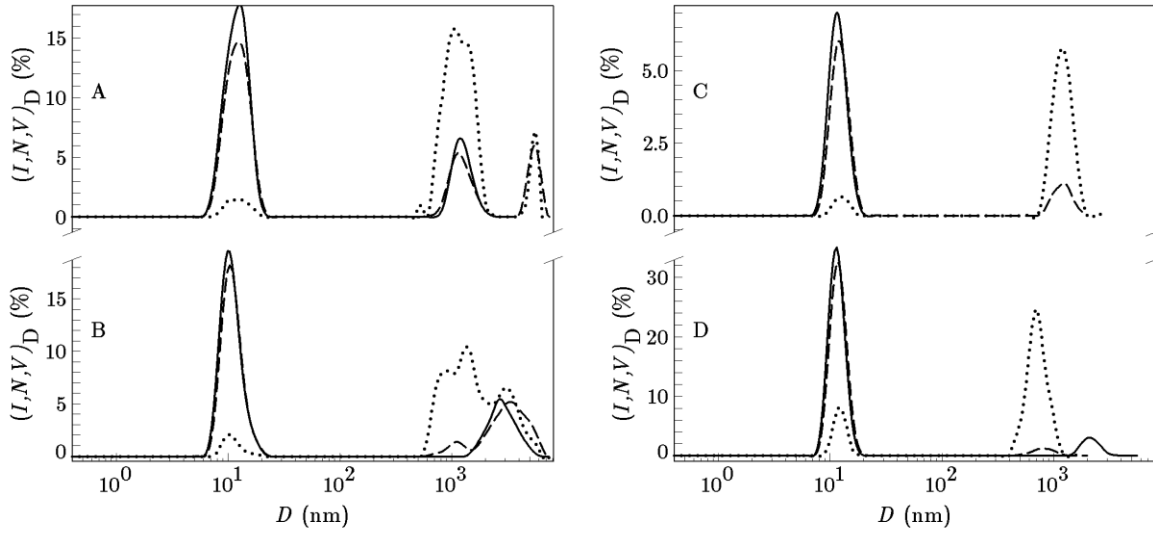


Fig. S4 DLS-PSDs by number (solid curves), volume (dashed curves) and intensity (dotted curves) of the 1aS-HmRM, characterized by $x_s = 0.0072$, and $R_S = x_s/0.36 = 0.02$, stirred/aged at room temperature for $t_s' = 40$ min (A), $t_s' = 80$ min (B), $t_s' = 120$ min (C) and $t_{A'} = 24$ h (D), after the addition of NaOH into the NaOH-free 1a-HmRM. t_s' is the time of *rt* stirring passed after the addition of NaOH into NaOH-free 1a-HmRM and $t_{A'} = t_s' + t_a'$, where t_a' is the time of additional *rt* aging under static conditions (see Experimental in the main text). N_D is the number percentage, V_D is the volume (mass) percentage and I_D is the scattering intensity percentage of the particles having the spherical equivalent diameter D .

Further increase of x_s and R_s , respectively, increases the rate of nanoparticles aggregation, by the reasons explained in the main text. The consequence is, that for $x_s = 0.0036$ and $R_s = [\text{NaOH}] / ([\text{NaOH}] + [\text{TPAOH}]) = x_s / 0.36 = 0.0036 / 0.36 = 0.01$, the dominant particle population [$D_p(N) = D_p(V) \approx 10 \text{ nm}$], is established at $t_s \leq 40 \text{ min}$ (Fig. S3A). The peak size of the dominant particle population ($\approx 10 \text{ nm}$) does not considerably change during the *rt* ageing of the 1aS-HmRM from $t_s \leq 40 \text{ min}$ (Fig. S3A) to $t_A = 24 \text{ h}$ (Fig. S3D). However, a partial disaggregation of the $\approx 10 \text{ nm}$ -sized aggregates into $\approx 3.5 \text{ nm}$ -sized aggregates (Figs. S3C and S3D), indicate that the system is not quite „stabilized“ during its *rt* ageing in the time interval from $t_s \leq 120 \text{ min}$ to $t_A = 24 \text{ h}$. It is reasonable to assume that the $\approx 3.5 \text{ nm}$ -sized aggregates represent the transitive population towards its disaggregation into the PNPs. The reason for the disaggregation and its possible mechanism are discussed and explained in the main text as well as later, in this section.

The particles population with $D_p(N) = D_p(V) \approx 10 \text{ nm}$ is dominant also for $R_s = x_s / 0.36 = 0.0072 / 0.36 = 0.02$ at least to $t_A = 24 \text{ h}$ (Fig. S4). However, in difference to the 1bS-HmRM with $x_s = 0.0036$ (Fig. S3), a part of the nanoparticles ($N_D \approx 23 \%$) exist in the form of aggregates characterized by $D_p(N) = D_p(V) \approx 1150 \text{ nm}$ even at $t_s \leq 40 \text{ min}$ (Fig. S4A). This indicates that the starting (at $t_s \leq 40 \text{ min}$) amount of the subsequently added Na^+ ions is sufficient not only for the aggregation of PNPs into $\approx 10 \text{ nm}$ -sized aggregates, but also for the aggregation of the 10 nm-sized aggregates to the much larger, $\approx 1000 \text{ nm}$ -sized, ones. Prolonged *rt* stirring from $t_s = 40 \text{ min}$ (Fig. S4A) to $t_s = 80 \text{ min}$ (Fig. S4B) does not influence the size and the number fraction of the dominant particle population [$D_p(N) = D_p(V) \approx 10 \text{ nm}$ and $N_D \approx 74 \%$ at $t_A = 80 \text{ min}$ (Fig. S4B)], but causes the increase of the size of the aggregates from $D_p(N) = D_p(V) \approx 1150 \text{ nm}$ at $t_s \leq 40 \text{ min}$ (Fig. S4A) to $D_p(N) \approx 2700 \text{ nm}$ and $D_p(V) \approx 3600 \text{ nm}$ at $t_s = 80 \text{ min}$ (Fig. S4B). Here is interesting that, in spite of the large size of the aggregates [$D_p(N) \approx 1200 \text{ nm} - 2700 \text{ nm}$], they do not precipitate. In addition, although the large aggregates are homogeneously dispersed (distributed) in the solution, the 1bS-HmRMs remain clear and transparent. As already mentioned in the main text, this indicates that the large particles represent low-density, rickety-held aggregates of $\approx 10 \text{ nm}$ -sized particles (aggregates of the PNPs). The disaggregation of the most of the large aggregates [$D_p(N) \approx 2700 \text{ nm}$ and $D_p(V) \approx 3600 \text{ nm}$] to the smaller ones [$D_p(N) = D_p(V) \approx 10 \text{ nm}$] in the time interval from $t_s = 80 \text{ min}$ (Fig. S4B) to $t_s = 120 \text{ min}$ (Fig. S4C), confirms this indication.

In difference to a slow aggregation at $x_s = 0.0072$ ($R_s = 0.02$), which results in the formation of ≈ 10 nm-sized aggregates as the dominant particles population (see Fig. S4), a relatively small increase of the amount of the subsequently added NaOH (from $R_s = 0.02$ to $R_s = 0.03$) causes immediate formation of large aggregates: The 1aS-HmRM contains ≈ 94 % (by number; ≈ 70 % by volume) of the particles (aggregates) with $D_p(N) = 1100$ nm and ≈ 6 % (by number; ≈ 30 % by volume) of the particles (aggregates) with $D_p(N) = 3600$ nm (see Fig. S5A).

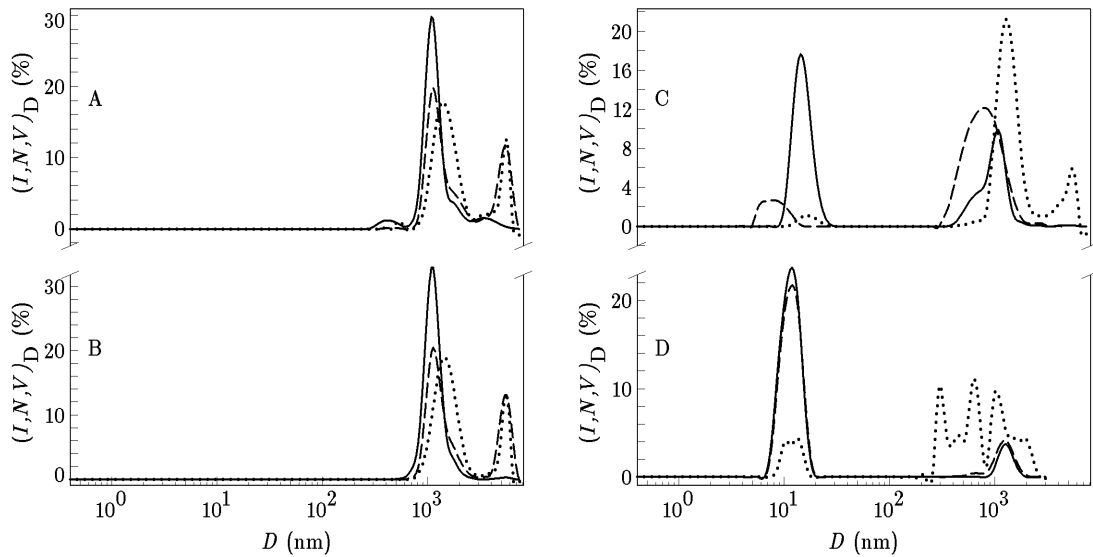


Fig. S5 DLS-PSDs by number (solid curves), volume (dashed curves) and intensity (dotted curves) of the 1aS-HmRM, characterized by $x_s = 0.0108$ and $R_s = x_s/0.36 = 0.03$, stirred/aged at room temperature for $t_{A'} = 40$ min (A), $t_{A'} = 120$ min (B), $t_{A'} = 24$ h (C) and $t_{A'} = 8$ d (D), after the addition of NaOH into the 1a-HmRM. t_s is the time of *rt* stirring passed after the addition of NaOH into NaOH-free 1a-HmRM and $t_{A'} = t_s + t_{a'}$, where $t_{a'}$ is the time of additional *rt* aging under static conditions (see Experimental in the main text). N_D is the number percentage, V_D is the volume (mass) percentage and I_D is the scattering intensity percentage of the particles having the spherical equivalent diameter D .

The rapid starting aggregation indicates that the added amount of Na^+ ions (3 mol % relative to total amount of cations, i.e., $\text{Na}^+ + \text{TPA}^+$) is sufficient for the removal of the TPA^+ ions from the PNPs shells (see Schemes 1C1 and 1C2 in the main text). This makes the conditions for efficient establishing of the $\equiv\text{Si}-\text{O}-\text{Si}\equiv$ bridges between colliding PNPs (see Scheme 1D in the main text) as well as for the prevention of disaggregation of the formed aggregates in the time interval from $t_s = 40$ min to $t_s = 120$ min (Figs. S5A and S5B). The large aggregates

formed at $t_s' \leq 40$ min are stable to at least $t_s' = 120$ min (see Figs. S5A and S5B). Then (at $t_s' > 40$ min), the large aggregates, start to disaggregate into ≈ 10 nm-sized aggregates at $t_s' > 120$ min. The consequence is that the 1aS-HmRM contains 60 % (by number) of the ≈ 10 nm-sized aggregates and 40 % (by number) of the ≈ 1000 nm-sized aggregates at $t_{A'} = 24$ h (Fig. S5C; also see Fig. 1D in the main text). Now, taking into consideration that the ≈ 1000 nm-sized aggregates are composed of the ≈ 10 nm-sized aggregates, and that the processes of aggregation and disaggregation are in dynamic equilibrium, it is reasonable to assume that a very small fraction of the ≈ 10 nm-sized aggregates coexists with the ≈ 1000 nm-sized aggregates even at $t_s' = 120$ min: While for $R_s = 0.02$, the fraction of the ≈ 10 nm-sized aggregates, which coexist with the about 1000 nm-sized aggregates is evident (see Figs. S4A and S4B), the ≈ 10 nm-sized aggregates cannot be detected by DLS for $R_s = 0.03$ (see Fig. S5), because of their very small fraction. Moreover, assuming that a part of the Na^+ ions associated with the deprotonated surface silanol groups (see Scheme 1C2) penetrates into nanoparticle's core during the prolonged stirring/aging, the negative charge of the deprotonated surface silanol groups becomes uncompensated. The uncompensated silanol groups may be compensated again by the TPA^+ ions from solution. In this way, the nanoparticles are stabilized again (see the corresponding discussion in the main text) and excluded from the aggregation process (formation of the ≈ 1000 nm-sized aggregates). Since, on the other hand, the processes of aggregation and disaggregation are in dynamic equilibrium, the excluded, ≈ 10 nm-sized aggregates are replaced by the disaggregation of the larger, ≈ 1000 nm-sized aggregates. The process of disaggregation takes place until a new dynamic equilibrium is established.

As already pointed out in the main text, from the results presented in Figs. 1B, 1C and 1D and Figs. S2 – S5 is evident that, although, the aggregates, existing in different 1aS-HmRMs ($x_s = 0.0018$, $x_s = 0.0036$, $x_s = 0.0072$ and $x_s = 0.0108$), have almost the same size at $t_{A'} = 24$ h [$D_p(N) \approx 10$ nm; see Figs. S2B, S3D, S4D and S5C], the “history” of the formation of these aggregates is different: For $x_s = 0.0018$ and $x_s = 0.0036$, the ≈ 10 nm-sized aggregates, are most probably formed by a stepwise aggregation of the PNPs. For $x_s = 0.0072$, the dominant, ≈ 10 nm-sized aggregates (76 % by number) coexists with the large, ≈ 1000 nm-sized aggregates (24 % by number) at $t_s' = 40$ min. This indicates that a part of the 10 nm-sized aggregates is immediately (at $t_s' \leq 40$ min) aggregated to the ≈ 1000 nm-sized aggregates (see Fig. S4). However, the formed large aggregates [$D_p(N) \approx 1000$ nm] are not stable and disaggregate again into the ≈ 10 nm-sized aggregates in the time interval from $t_s' = 40$ min to

$t_s = 120$ min. Thereafter, the 10 nm-sized aggregates are stable to at least $t_{A'} = 24$ h (see Fig. S4). The increase of the amount of the subsequently added NaOH from $x_s = 0.0072$ to $x_s = 0.0108$ causes very fast and intensive aggregation processes, so that only the aggregates with $D_p(N) \approx 1000$ nm are present in the 1aS-HmRM at $40 \text{ min} \leq t_s \leq 120 \text{ min}$ (see Figs. S5A and S5B). However, similarly as for $x_s = 0.0072$, the large aggregates are not stable, so that most of them disaggregate into the “starting” ≈ 10 nm sized particles (aggregates) in the time interval from $t_s = 120$ min (Fig. S4B) to $t_{A'} = 24$ h (Fig. S4C);

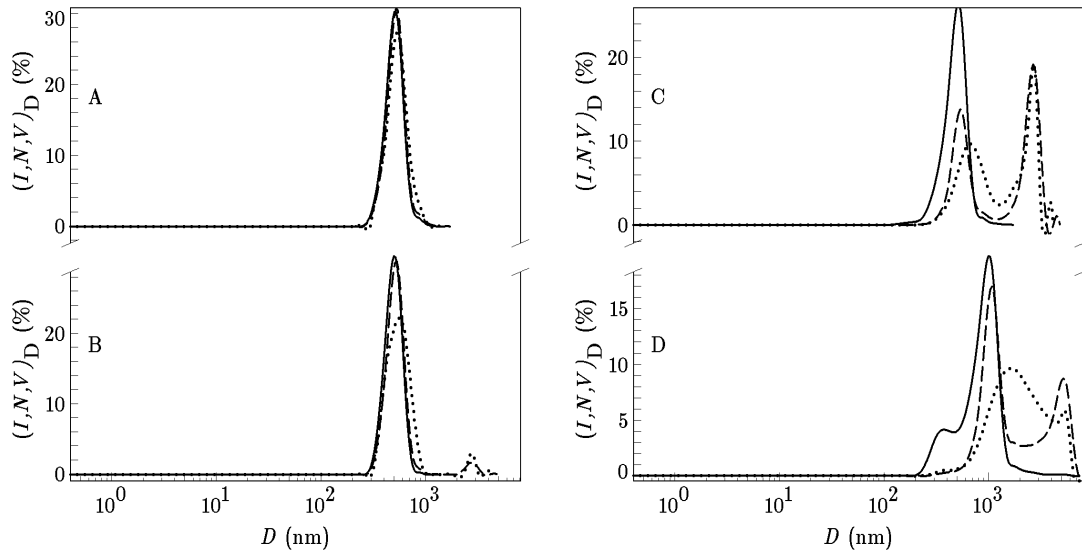


Fig. S6 DLS-PSDs by number (solid curves), volume (dashed curves) and intensity (dotted curves) of the 1aS-HmRM, $x_s = 0.0144$ and $R_s = x_s/0.36 = 0.04$, stirred/aged at room temperature for $t_s = 40$ min (A), $t_{A'} = 24$ h (B), $t_{A'} = 4$ d (C) and $t_{A'} = 8$ d (D), after the addition of NaOH into the 1a-HmRM. t_s is the time of *rt* stirring passed after the addition of NaOH into NaOH-free 1a-HmRM and $t_{A'} = t_s + t_a$, where t_a is the time of additional *rt* aging under static conditions (see Experimental in the main text). N_D is the number percentage, V_D is the volume (mass) percentage and I_D is the scattering intensity percentage of the particles having the spherical equivalent diameter D .

At $t_{A'} = 24$ h, 60 % of particles belongs to the population with $D_p(N) \approx 10$ nm and 40 % of particles belong to the population with $D_p(N) \approx 1000$ nm (Fig. S5C; also see Fig. 1D in the main text). The process of disaggregation continued during the prolonged *rt* aging so that 90 % of particles belong to the population with $D_p(N) \approx 10$ nm and 10 % of particles belongs to the population with $D_p(N) \approx 1000$ nm at $t_{A'} = 8$ d (see Fig. S5D in SI-2).

Finally, for $x_s \geq 0.0144$, the size of the large particles [$D_p(N) = D_p(V) = D_p(I) \approx 500$ nm], formed at $t_s \leq 40$ min (Fig. S6A) do not considerable change during the *rt* stirring from $t_s =$

40 min to $t_s = 120$ min and during the *rt* ageing under static conditions from $t_s = 120$ min to $t_A = 24$ h (Fig. S6B; also see Fig. 1E in the main text). While, the particle size distribution by number does not change during the prolonged *rt* aging under static conditions from $t_A = 24$ h (solid curve in Fig. S6B) to $t_A = 4$ d (solid curve in Fig. S6C), the particle size distributions by volume (mass) and intensity split into two separate particles populations [$D_p(V)_1 = 550$ nm, $V_{D-1} = 53$ % and $D_p(V)_2 = 2800$ nm, $V_{D-2} = 47$ %; $D_p(I)_1 = 640$ nm, $V_{D-1} = 51$ % and $D_p(I)_2 = 2800$ nm, $V_{D-2} = 49$ %], during the same time interval (dashed and dotted curves in Figs. S6B and S6C). These, together with the increase of the particles size from $D_p(N) \approx 500$ nm at $t_A = 4$ d min (Fig. S6c) to $D_p(N) \approx 1000$ nm at $t_A = 8$ d (Fig. S6D), point out to the intensive aggregation processes during the long-time *rt* ageing under static conditions. The absence of the disaggregation processes indicates that for $x_s \geq 0.0144$, the amount (concentration) of the Na^+ ions in the liquid phase is large enough to prevent the re-stabilization of the nanoparticles by TPA^+ ions from solution, as it is explained in the main text.

In difference to preparation of the Na^+ -containing 1aS-HmRMs by subsequent addition of NaOH into the Na^+ -free 1a-HmRMs (1a-HmRMs + $\text{NaOH} \rightarrow$ 1aS-HmRMs; see Experimental in the main text), the preparation of the Na^+ -containing 2D-HmRMs by a direct addition of NaOH (see Experimental in the main text), is consistent with the preparation of most HmRMs in the systems: $\text{SiO}_2\text{-NaOH-TPAOH-EtOH-H}_2\text{O}$,^{4,14,25,33,A5-A9} but also with the preparation of heterogeneous systems.^{40,44,45,A10-A12}

Figure S7A shows that the nanoparticles, formed in the 2D-HmRM ($x_d = 0.018$, $R_d = x_d/0.36 = 0.05$) at $t_s \leq 40$ min, are characterized by $D_{\min}(N) \approx 1$ nm, $D_{\max}(N) \approx 3.5$ nm and $D_p(N) = 1.74$, which is typical for the primary nanoparticles – PNPs (see the main text). The sizes of the PNPs, formed at $t_s \leq 40$ min, does not considerably change during the prolonged *rt* aging under static conditions, at least to $t_A = 29$ days (Fig. S7C). This stability, comparable with the stability of the PNPs formed in the absence of Na^+ ions (compare Figs. S1 and S7), is discussed and explained in the main text. Appearance of the „particles“ population characterized by $D_{\min}(N) = 0.54$ nm, $D_{\max}(N) = 0.96$ nm and $D_p(N) = 0.83$ nm at $t_A = 29$ days (Fig. S7C), indicates that a part of the PNPs has been decomposed into polysilicate anions⁵¹ during the prolonged *rt* aging from $t_A \geq 24$ h to $t_A \leq 29$ days.

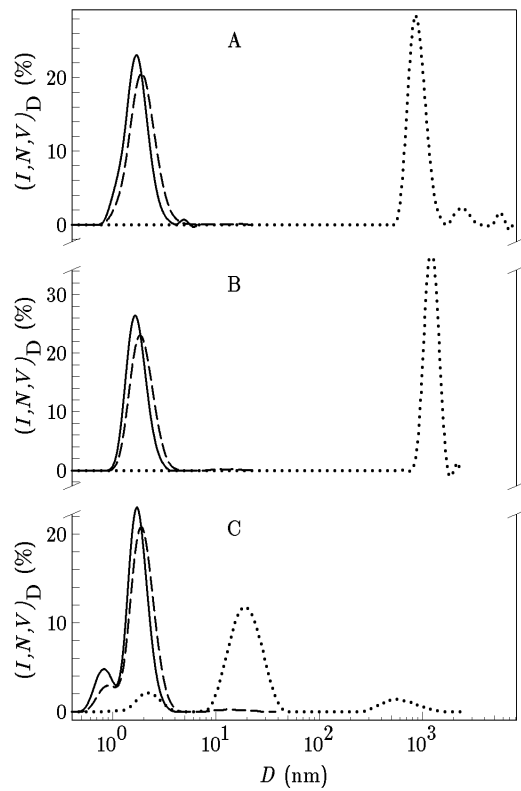


Fig. S7 DLS-PSDs by number (solid curves), volume (dashed curves) and intensity (dotted curves) of the 2D-HmRM, characterized by $x_d = 0.018$, and $R_d = x_d/0.36 = 0.05$, stirred/aged at room temperature for $t_s = 40$ min (A), $t_A = 24$ h (B) and $t_A = 29$ d (C). NaOH is added to the reaction mixture in a direct way (see Experimental in the main text). t_s is the time of stirring of the reaction mixture after the addition of TEOS to the water solution of TPAOH and NaOH and $t_A = t_s + t_a$, where t_a is the time of additional *rt* aging under static conditions (see Experimental in the main text). N_D is the number percentage, V_D is the volume (mass) percentage and I_D is the scattering intensity percentage of the particles having the spherical equivalent diameter D .

For $R_d = 0.075$ ($x_d = 0.027$), the PNPs [$D_{\min}(N) \approx 1$ nm, $D_{\max}(N) \approx 4.2$ nm and $D_p(N) = 1.74$; $N_D = 83$ %], formed at $t_s \leq 40$, coexists with a small fraction (17 % by number) of the particles“ having the sizes in the range from about 0.46 to about 0.96 nm. As already has been assumed, these “particles”, smaller than 1 nm, possibly correspond to the polysilicate anions (oligomers) associated with TPA^+ ions or even the core@shell particles at the early stage of the formation.⁵¹ The particles populations, formed at $t_s \leq 40$ min, do not considerably change during the *rt* stirring from $t_s = 40$ min (Fig. S8A) to $t_s = 120$ min (Fig. S8B). Then, the particle size slightly increases, so that $D_p(N) \approx 2$ nm at $t_A = 24$ h; however, a small fraction (≈ 10 % by number) of the sub-nanometre-sized “particles“ [$(D_p(N) \approx 0.6$ nm)] coexists with the PNPs and their small aggregates (see Fig. 1B in the main text).

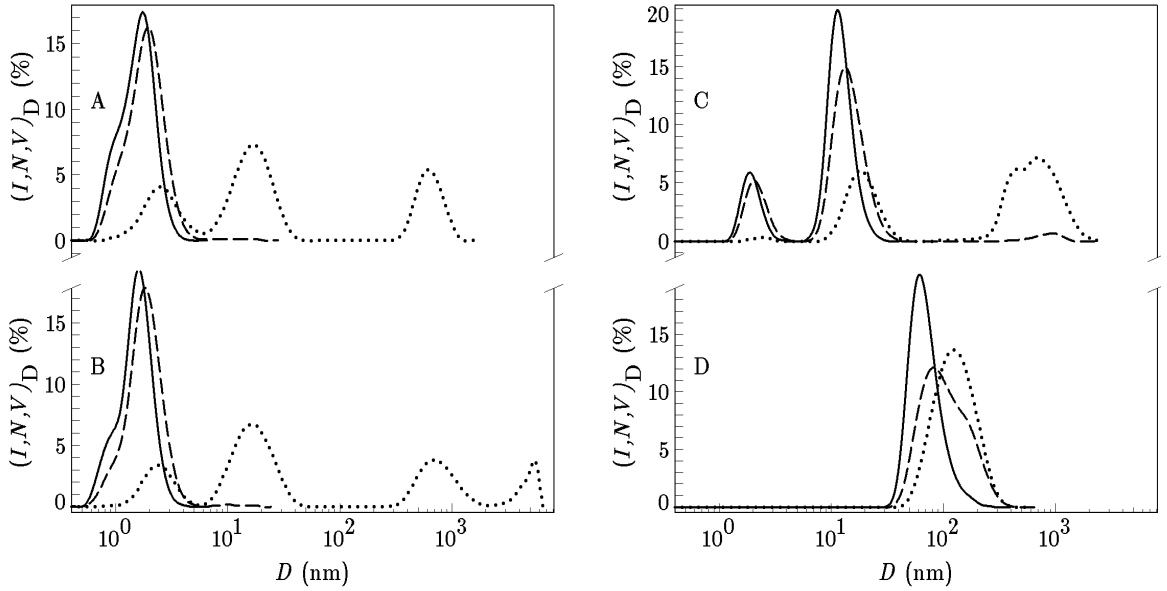


Fig. S8 DLS-PSDs by number (solid curves), volume (dashed curves) and intensity (dotted curves) of the 2D-HmRM, characterized by $x_d = 0.027$ and $R_d = x_d/0.36 = 0.075$, stirred/aged at room temperature for $t_s = 40$ min (A), $t_s = 120$ min (B), $t_A = 8$ d (C) and $t_A = 28$ d (D). NaOH is added to the reaction mixture in a direct way (see Experimental in the main text). t_s is the time of stirring of the reaction mixture after the addition of TEOS to the water solution of TPAOH and NaOH and $t_A = t_s + t_a$, where t_a is the time of additional *rt* aging under static conditions (see Experimental in the main text). N_D is the number percentage, V_D is the volume (mass) percentage and I_D is the scattering intensity percentage of the particles having the spherical equivalent diameter D .

The prolonged *rt* ageing of the 2D-HmRM ($x_d = 0.027$, $R_d = 0.075$) causes gradual aggregation of the PNPs into larger particles (aggregates), so that ≈ 20 % of the particles have the size, $D_p(N) \approx 2$ nm, which is close to the size of the PNPs, and ≈ 80 % of the particles exist in the form of their aggregates, with $D_p(N) \approx 12$ nm, at $t_A = 8$ d (Fig. S8C). The process of aggregation continues, so that all nanoparticles exist in the form of larger aggregates, with $D_p(N) \approx 60$ nm, at $t_A = 28$ d (Fig. S8D).

An increase of the Na^+ content, additionally decreases the stability of the PNPs, as it is indicated by the gradual increase of the particles size (expressed by the „peak“ size, D_p). For $R_d = 0.1$ ($x_d = 0.036$), the PNPs [$D_p(N) \approx 1.7$ nm] are stable at $t_s = 40$ min (Fig. S9A) and then, the particles size increases from $D_p(N) = 2.3$ nm at $t_s = 80$ min (Fig. S9B), through $D_p(N) = 2.7$ nm at $t_s = 120$ min (Fig. S9C), min, $D_p(N) = 11.7$ nm at $t_A = 24$ h (Fig. S9D; also see Fig. 1C' in the main text) to $D_p(N) = 78$ nm at $t_A = 8$ d (Fig. S9E).

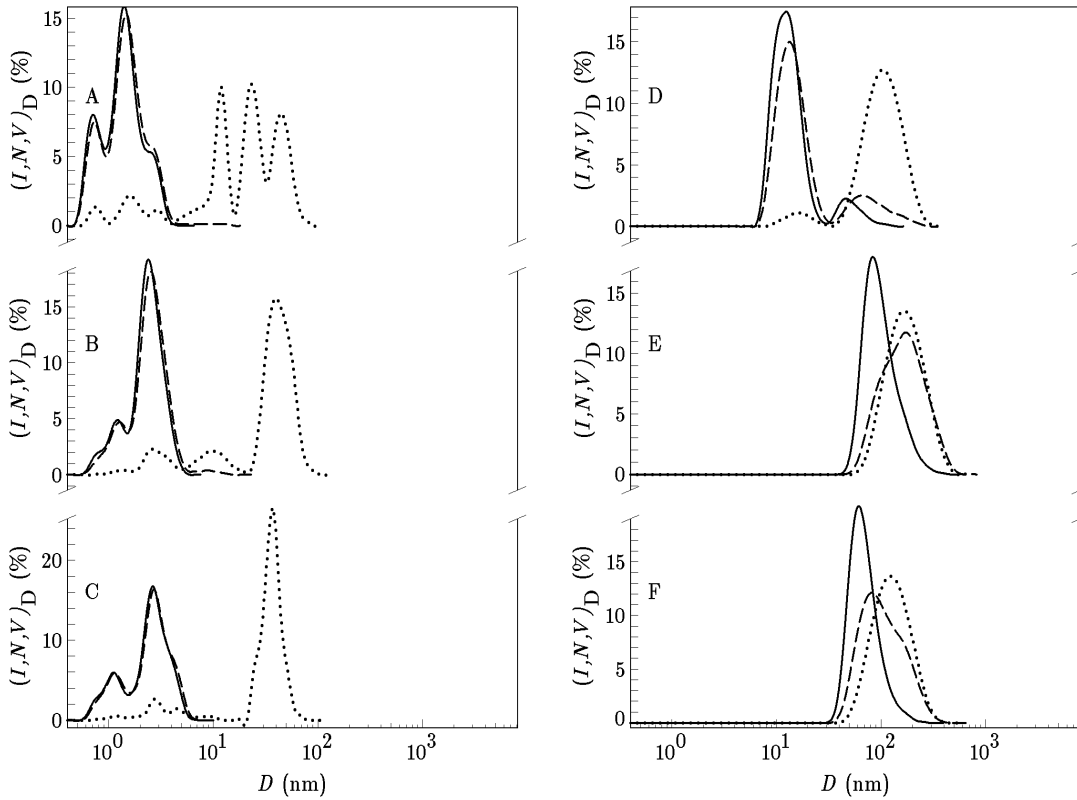


Fig. S9 DLS-PSDs by number (solid curves), volume (dashed curves) and intensity (dotted curves) of the 2D-HmRM, characterized by $x_d = 0.036$ and $R_d = x_d/0.36 = 0.1$, stirred/aged at room temperature for $t_s = 40$ min (A), $t_s = 80$ min (B), $t_s = 120$ min (C), $t_A = 24$ h (D), $t_A = 8$ d (E) and $t_A = 28$ d (F). NaOH is added to the reaction mixture in a direct way (see Experimental in the main text). t_s is the time of stirring of the reaction mixture after the addition of TEOS to the water solution of TPAOH and NaOH and $t_A = t_s + t_a$, where t_a is the time of additional *rt* aging under static conditions (see Experimental in the main text). N_D is the number percentage, V_D is the volume (mass) percentage and I_D is the scattering intensity percentage of the particles having the spherical equivalent diameter D .

Thereafter, the particle size slightly decreases during the further room temperature ageing of the 2D-HmRM ($x_d = 0.036$, $R_d = 0.1$), so that $D_p(N) = 58$ nm at $t_A = 28$ d (see Fig. S9F). As already is explained in the main text, the complete amount of the Na^+ ions is incorporated in the nanoparticle core during its formation, when the Na^+ ions are added directly (as NaOH) in the 2D-HmRMs with $R_d = 0.05$ ($x_d = 0.018$) (see Scheme 3A in the main text). It can be assumed, that in this case, there are no “free” Na^+ ions which could be able to remove the TPA^+ ions from the nanoparticle shell (see Schemes 1C1 and 1C2 in the main text) and thus, to initiate the aggregation processes by the formation of the $\equiv\text{Si}-\text{O}-\text{Si}\equiv$ linkages between the collided PNPs (see Schemes 1B, 1D and 1E in the main text). This, together with the negative charge of the PNPs,^{31,35,50,63} is the reason that the PNPs are stable

during the long-time *rt* ageing (Fig. S7). On the other hand, although almost the complete amount of the Na^+ ions is incorporated in the nanoparticle's core for $R_d = 0.075$ ($x_d = 0.027$) and $R_d = 0.1$ ($x_d = 0.036$), respectively, it seems that a small fraction of the added Na^+ ions is not incorporated into the nanoparticle core immediately (see Schemes 3B and 3C in the main text). These “free” Na^+ ions can remove the equivalent amount of the TPA^+ ions from the nanoparticle shell (see Schemes 1C1 and 1C2 in the main text) and thus, make possibilities for the limited formation of the $\equiv\text{Si}–\text{O}–\text{Si}\equiv$ linkages between the collided PNPs (see Scheme 1D in the main text). This causes a slow process of aggregation during long-time *rt* ageing under static conditions. The size of aggregates increases from $D_p(\text{N}) \approx 2 \text{ nm}$ at $t_A = 24 \text{ h}$ (Fig. 1B' in the main text), through $D_p(\text{N})-1 \approx 2 \text{ nm}$ and $D_p(\text{N})-2 \approx 12 \text{ nm}$ at $t_A = 8 \text{ d}$ (Fig. S8C) to $D_p(\text{N}) \approx 60 \text{ nm}$ at $t_A = 28 \text{ d}$ (Fig. S8D).

Since there is no doubt that the increase of x_d and R_d , respectively, increases the fraction of the “free” Na^+ ions (see Scheme 3 in the main text), a higher rate of aggregation in the 2D-HmRM with $R_d = 0.1$ ($x_d = 0.036$) (Fig. S9), relative to the rate of aggregation in the 2D-HmRM with $R_d = 0.075$ ($x_d = 0.027$) (Fig. S8) was expected. However, in spite of different rates of aggregation, the final (“equilibrium”) size of the aggregates is almost the same [$(D_p(\text{N}) \approx 60 \text{ nm})$] for both the 2D-HmRMs.

A comparison of Figs. S9 and S10 shows that a small increase in NaOH content, i.e., from $x_d = 0.036$ to $x_d = 0.0396$ ($\Delta x_d = 0.0036$, $\Delta R_d = 0.01$) considerably accelerates the aggregation of the PNPs into the larger particles (aggregates). While for $x_d = 0.036$, the PNPs are stable at least to $t_s = 40 \text{ min}$ (Fig. S9A) and then, gradually aggregate into larger aggregates (Figs. 9B – 9F), for $x_d = 0.0396$, the PNPs gradually aggregate to the aggregates, characterized by $D_p(\text{N}) = 90 \text{ nm}$ and $D_p(\text{V}) = D_p(\text{I}) = 164 \text{ nm}$ at $t_A \leq 40 \text{ min}$ (Fig. S10A). Prolonged *rt* ageing under static conditions, increases the size of aggregates to $D_p(\text{N}) = 164 \text{ nm}$, $D_p(\text{V}) = 342 \text{ nm}$, and $D_p(\text{I}) = 255 \text{ nm}$ at $t_A = 24 \text{ h}$ (see Fig. 1D' in the main text). Thereafter, the particles size distributions, established at $t_A = 24 \text{ h}$, do not change during the prolonged *rt* ageing, at least to $t_A = 28 \text{ d}$ (Fig. S9C). This, rapid increase of the rate of aggregation, when x_d increases from 0.036 to 0.0396 (R_d increases from 0.1 to 0.11), is obviously caused by the increase of the amount (concentration) of “free” Na^+ ions, which are able to remove the TPA^+ ions from the nanoparticle shell (see Schemes 3C and 3D in the main text). Then, the removed TPA^+ ions are, in the nanoparticle shell, substituted by smaller Na^+ ions (see Schemes 1C1 and 1C2 in the main text).

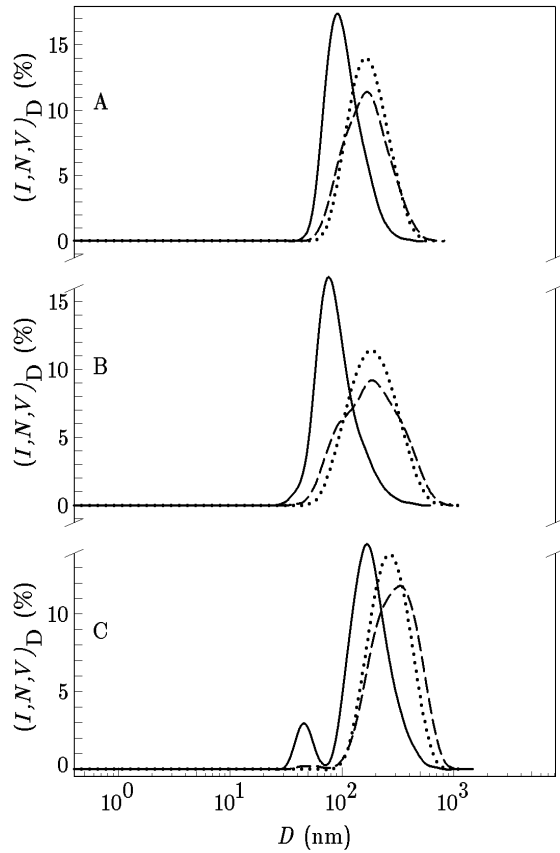
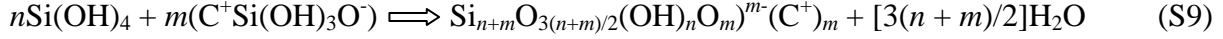


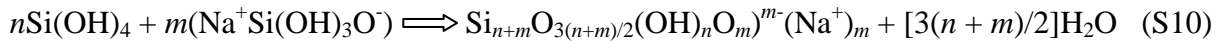
Fig. S10 DLS-PSDs by number (solid curves), volume (dashed curves) and intensity (dotted curves) of the 2D-HmRM, characterized by $x_d = 0.0396$, and $R_d = x_d/0.36 = 0.11$, stirred/aged at room temperature for $t_s = 40$ min (A), $t_s = 120$ min (B) and $t_A = 28$ d (C). NaOH is added to the reaction mixture in a direct way (see Experimental in the main text). t_s is the time of stirring of the reaction mixture after the addition of TEOS to the water solution of TPAOH and NaOH and $t_A = t_s + t_a$, where t_a is the time of additional *rt* aging under static conditions (see Experimental in the main text). N_D is the number percentage, V_D is the volume (mass) percentage and I_D is the scattering intensity percentage of the particles having the spherical equivalent diameter D .

This substitution causes exposition of a part of the terminal silanol groups to the liquid phase (see Schemes 1C2 and 3 in the main text) and thus, makes them disposable for the formation of the $\equiv\text{Si}-\text{O}-\text{Si}\equiv$ linkages between the collided PNPs and their aggregates [see Eq. (1) in the main text]. The increase of the amount of “free” Na^+ ions at $x_d = 0.0396$ ($R_d = 0.11$), indicates that there is a „threshold“ amount of the Na^+ ions [defined by $x_d(\text{tr})$ and $R_d(\text{tr})$, respectively] which can be incorporated into the nanoparticle core. Each „excess“ ($R_d > 0.1$, $x_d > 0.036$) of the Na^+ ions acts as the subsequently added Na^+ ions (see Schemes 3D and 3E). The „threshold“ amount of Na^+ ions is probably closely related to the mechanism by which the Na^+ ions are incorporated to the nanoparticle core: In the main text is postulated that that the

Na^+ ions are in the nanoparticle core introduced as the $\text{Si}(\text{OH})_3\text{O}^{\cdots\cdots\cdots}\text{Na}$ species, formed during the hydrolysis of TEOS [see Eq. (2) in the main text]. This can be realized by the reactions of the $\text{Si}(\text{OH})_3\text{O}^{\cdots\cdots\cdots}\text{Na}$ species, and the $\text{Si}(\text{OH})_4$ monomers formed above the CAC (SI-1), e.g.,

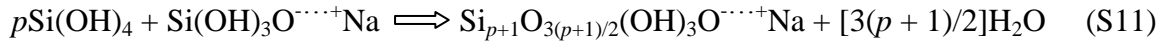


where C^+ is a cation. However, if the original equation, in which $\text{C}^+ = \text{TPA}^+$, is taken literally,⁴⁷ the SiO_2 core and TPA^+ shell would not appear as distinct entities, but the entire nanoparticle would be composed of more or less homogeneously distributed $\text{Si}_{n+m}\text{O}_{3/2(n+m)}(\text{OH})_n\text{O}_m)^{m-}(\text{TPA}^+)_m$ entities. This is, in contrast with the finding that the nanoparticle core is TPA-free.⁴⁸ A possible reason is that the TPA^+ ion is too large to be positioned in the nanoparticle core. On the other hand, if the above relationship implies formation of the nanoparticle core by the mutual reactions of the $\text{Si}(\text{OH})_4$ monomers formed above the CAC,^{34,35,54} and subsequent “attachment” of the $\text{Si}(\text{OH})_3\text{O}^{\cdots\cdots\cdots}\text{TPA}$ units on the surface of the nanoparticle core, such formed nanoparticles would have a core@shell structure; however in that case, the TPA^+ ions would not be directly adsorbed on the surface of the nanoparticle core,^{17,27-29,35,37,53-56} but on the $(\text{NP})\text{Si}-\text{O}-\text{Si}(\text{OH})_2\text{O}^-$ group,⁵² where $(\text{NP})\text{Si}-$ is the surface Si of the nanoparticle core. Finally, if the reaction mixture contains Na^+ ions during the hydrolysis of TEOS (e.g., if NaOH is added directly), then a part of the deprotonated silicate monomers $[\text{Si}(\text{OH})_3\text{O}^-]$ would be associated with Na^+ ions, i.e., $\text{C}^+ = \text{Na}^+$ in Eq. (S9). In this case, it can be assumed that the fraction of $\text{Si}(\text{OH})_3\text{O}^{\cdots\cdots\cdots}\text{Na}$ units is proportional to x_d and R_d , respectively. Now, taking into consideration that Na^+ ion is small enough to be positioned in the nanoparticle core, a replacement of C^+ with Na^+ in Eq. (S9), gives,



Furthermore, assuming that the „threshold“ amount of the Na^+ ions, which can be incorporated into nanoparticle core, is defined with $x_d(\text{tr}) \approx 0.036$ and $R_d(\text{tr}) \approx 0.1$ (see the main text), it can be easily calculated that the „threshold“ ratio Si/Na in the nanoparticle core

is about 28. This means that $\approx 3.6\%$ of Si atoms in the nanoparticle core can be associated with Na^+ ions ($\equiv\text{Si}-\text{O}^{\cdots\cdots+}\text{Na}$). In this case, the equation (10) can be rewritten as,



where $p \leq 28$. Here it is interesting that the percentage of Si atoms ($\leq 3.6\%$), which can be in the nanoparticle core associated with Na^+ ions, is in the range of the percentage of Q^1 Si atoms (≈ 1 to $\approx 8\%$) in the amorphous cores of silica^{30,46,49,52} and aluminosilica^{15,21} nanoparticles. Here, Q^1 denotes the Si atoms linked by only one silicon atom, i.e., $\equiv\text{Si}-\text{O}-\text{Si}(\text{X})_3$, where $\text{X} = -\text{OH}$ and/or $-\text{O}^-$. This implies that the Na^+ ions, in the nanoparticle core, are associated with the deprotonated silanol groups of the “parent” Q^1 Si atoms. The “parent” Q^1 Si atoms are formed by realizing the cbp– $\text{Si}(\text{OH})_2-\text{O}^{\cdots\cdots+}\text{Na}$ linkage, where the “cbp” are the sites in the core bulk, where the $-\text{Si}(\text{OH})_3\text{O}^{\cdots\cdots+}\text{Na}$ species are positioned. As can be seen in the appropriate literature,^{15,21,30,46,49} the percentage of the Q^1 Si atoms, in the nanoparticle’s core, is not strongly fixed, but depends on the chemical composition of the reaction mixture. In this way, the “threshold” amount of Na^+ ions, incorporated to the nanoparticle core, is limited by the number of the places at which the $\text{Si}(\text{OH})_3\text{O}^{\cdots\cdots+}\text{Na}$ species can be attached. Although the above described mechanism of the incorporation of Na^+ ions to nanoparticle core cannot be directly proved, it is the most reasonable at present.

Finally, for $R_d \geq 0.13$ ($x_d = 0.0468$), the PNPs very fast (in less than 40 min) aggregate into ≈ 1000 nm sized aggregates (Fig. S11A). The particles formed at the early stage of aggregation ($t_s \leq 40$ min) do not change their sizes during the prolonged *rt* ageing, at least to $t_A = 28$ d (Fig. S11C). Here, it is interesting that the sizes of the aggregates formed for $R_d \geq 0.13$ and existing at $t_A = 24$ h (Figs. 1E' and 1F' in the main text), are comparable with the sizes of the aggregates formed for $R_s \geq 0.04$ ($x_s = 0.0144$) and existing at $t_A = 24$ h (Figs. 1E and 1F in the main text). In addition, it is interesting that the differences $(R_d = 0.13) - (R_s = 0.04) = 0.09$ and $(x_d = 0.0468) - (x_s = 0.0144) = 0.0324$ are close to the assumed „threshold“ values [$R_d(\text{tr}) \approx 0.1$ and $x_d(\text{tr}) \approx 0.036$; see the main text].

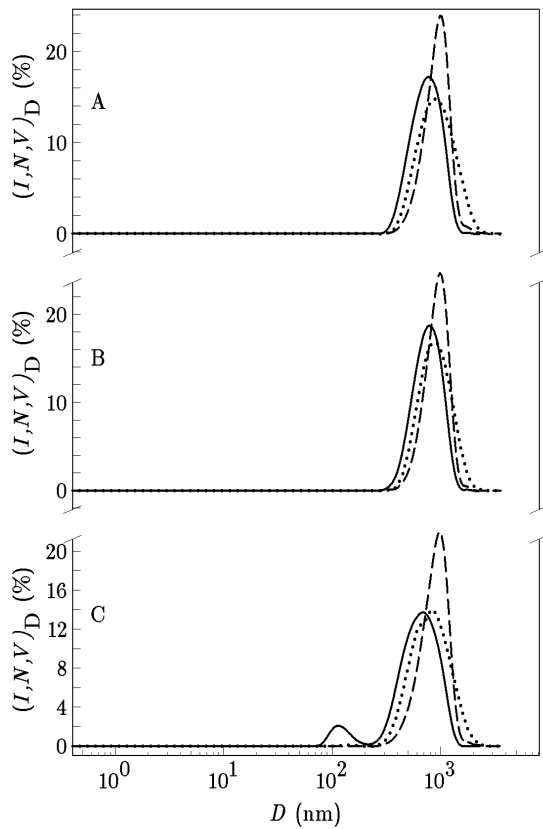


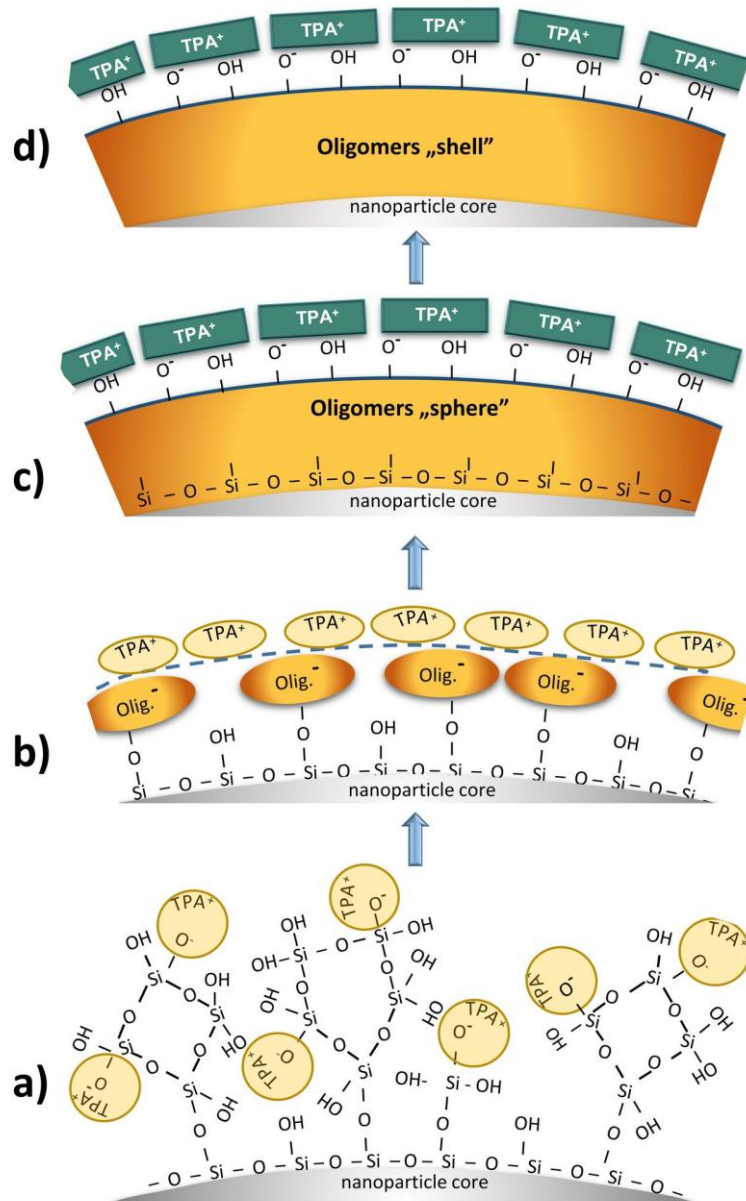
Fig. S11 DLS-PSDs by number (solid curves), volume (dashed curves) and intensity (dotted curves) of the 2D-HmRM characterized by $x_d = 0.0468$ and $R_d = x_d/0.36 = 0.13$, stirred/aged at room temperature for $t_s = 40$ min (A), $t_s = 120$ min (B) and $t_A = 28$ d (C). NaOH is added to the reaction mixture in a direct way (see Experimental in the main text). t_s is the time of stirring of the reaction mixture after the addition of TEOS to the water solution of TPAOH and NaOH and $t_A = t_s + t_a$, where t_a is the time of additional *rt* aging under static conditions (see Experimental in the main text). N_D is the number percentage, V_D is the volume (mass) percentage and I_D is the scattering intensity percentage of the particles having the spherical equivalent diameter D .

This additionally confirms the hypothesis that, above the „threshold“ amount of the directly added NaOH, the “excess” of the Na^+ ions are distributed outside of the nanoparticles (see Scheme 3 in the main text) and act in the same way as the subsequently added Na^+ ions (see Schemes 1C1, 1C2 and 1D in the main text).

SI-3: Simplification of schematic presentation of nanoparticle shell

Very often, the nanoparticle shell is considered as organic cations (Org^{n+}), usually tetraalkylammonium (TAA^+) and most frequently, TPA^+ ions, adsorbed on the surface of SiO_2 nanoparticle core.^{17,21,27-29,35,37,48,50,51,53,56} This consideration includes the association of the Org^{n+} (TAA^+ , TPA^+) ions with the deprotonated surface silanol groups³⁷ and formation of a Stern layer of the adsorbed cations, that is effectively part of the liquid phase of the system.^{27,35,50} However, recent investigation of the processes occurring during early stages of the formation and room temperature (*rt*) evolution of the core(amorphous SiO_2)@shell(organocations) nanoparticles has shown that, above the critical aggregation concentration (CAC) of SiO_2 , the nanoparticle shell can be formed by the attachment of the polysilicate anions (silicate oligomers), associated with TPA^+ ions, on the surfaces of the nanoparticles's cores.⁵² This gives a new insight in the “structure” of the nanoparticle’s shell, which is considerably different from the most frequently described one, i.e., “free” TPA^+ ions adsorbed on the surface of the nanoparticle’s core^{21,27-29,34} (see Scheme 1-V5 in Ref. 52 as well as Schemes S1a here and Scheme 2 in the main text). Because the complexity of the nanoparticle shell, the nanoparticles (primary nanoparticles – PNPs) are, in the main text, presented in simplified forms; nanoparticle core is surrounded with the (inner) “shell” of polysilicate anions (silicate oligomers) which is surrounded by the (outer) “shell” of tetrapropylammonium (TPA^+) ions (see Schemes 1, 3 and 4 in the main text); the TPA^+ ions are presented as “rounded bricks”. The steps of simplification are presented in Scheme S1: The nanoparticle shell is composed of mainly TPA^+ -bearing D4R and D5R oligomers and smaller fractions of the TPA^+ -bearing monomers and dimers (Scheme S1a).⁵² For the sake of simplicity, only the simplified, “2D sketches” of the TPA^+ -bearing D4R and D5R units are presented in the scheme (see Scheme S1a). For the same reason, the TPA^+ ions are presented by yellow circles (see Scheme S1a). The first step of the simplification is the presentation of both oligomers and TPA^+ ions by ellipsoids (see Scheme S1b). The oligomers (brown ellipsoids) are directly attached to the nanoparticle core by the core \equiv Si–O–Si-oligomer linkages, and TPA^+ ions (yellow ellipsoids) are associated with deprotonated silanol groups of oligomers (e.g., core \equiv Si–O– $\text{Si}_4\text{O}_4(\text{OH})_7\text{O}^{\cdots\cdots+}$ TPA; see Scheme S1a or core \equiv Si–O–olig $^{\cdots\cdots+}$ TPA; see Scheme S1b). However, since the “simplified” feature, presented in Scheme S1b, is still too complicated for the presentation of behaviour of the nanoparticles in the presence of Na^+ ions (see Schemes 1, 3 and 4 in the main text), the next

step of the simplification procedure resulted in the presentation of oligomers in the form of continuous layer (oligomers “sphere”) around the nanoparticle core and TPA^+ ions are presented as the “rounded bricks” (see Scheme S1c).



Scheme S1 Steps of the simplification of the nanoparticle shell. The steps are described in the text

Further (final) simplification includes the “vanishing” (hiding) of the terminal silanol groups of the nanoparticle core (see Schemes S1d as well as Schemes 1, 3 and 4 in the main text). Although the relative sizes and shapes of the nanoparticle “elements” (core, Si, O and H

atoms at the surface of nanoparticle core and in oligomers as well as TPA^+ ions) are not entirely realistic, the behaviour of the core(amorphous silica)@shell(TPA-polysilicates) nanoparticles (PPSs) in the presence of Na^+ ions, can be readily explained by the simplified presentation of the nanoparticles as it is shown in Schemes 1, 3 and 4 in the main text. Namely, TPA^+ ions overlay not only the directly interacting silanol groups of the attached oligomers, but also the surrounding ones;⁵² this is more exactly presented in the Scheme 1-Vb in Ref. 56 (also see Scheme 2 in the main text), and in a more simplified way in the Schemes 1C, 3 and 5A in the main text). In this way, the “terminal” silanol groups of the TPA-containing oligomers (shell) are unable for the formation of (new) $(\text{NP})\text{Si}–\text{O}–\text{Si}(\text{NP})$ linkages between eventually collided core@shell nanoparticles (NP) (see Schemes 1B, 1E, 2 and 4 in the main text).

SI-4: ^{29}Si -NMR analysis

Although the amounts of Si in the form of oligomers (Total_{olig} in Table S2) and their distributions are generally consistent with the results of previous investigations,^{15,16,21,30,46,49} the specific data in Table S2 show that a subsequent addition of NaOH to the Na-free HmRMs induces a decrease of Si amount (expressed as the wt. %) in the form of oligomers. This decrease is mostly accounted by the decrease of the fractions of monomers, double four (D4R) and double five (D5R) rings. Further increase of the amount of the subsequently added NaOH from $x_s = 0.0036$ to $x_s = 0.0144$ does not considerably change neither the total amount of Si in the form of oligomers nor its distribution (see the 3rd and 4th columns in Table S2). On the other hand, since for each HmRm, the sum of Total_{olig} (Table S2) and Total_{NP} (Table S3) is 100 %, it is evident that decrease of the Total_{olig}, after (subsequent) addition of NaOH into Na-free HmRM, is caused by a partial aggregation of some oligomers into nanoparticles.

Table S2 Distributions of Si, in the forms of silicate monomers and polysilicate anions (oligomers), in HmRM₀-I (A) and in 1aS-HmRMs, characterized by: $x_s = 0.0036$ (B) and $x_s = 0.0144$ (C). The weight percentage of Si, in the form of silicate monomers and different polysilicate anions (oligomers), is provided by the analysis of the corresponding ^{29}Si -NMR spectra in Figs. 3A – 3C in the main text. The ^{29}Si -NMR spectra of all the samples are recorded 24 h hours after preparation ($t_A = 24$ h for $x_s = x_d = 0$) or after subsequent addition of NaOH ($t_A = 24$ h for $x_s = 0.0036$ and $x_s = 0.0144$, respectively; see Experimental in the main text).

HmRM: $\text{SiO}_2:x_s\text{NaOH}(0.36 - x_s)\text{TPAOH:4EtOH:18H}_2\text{O}$			
(poly)silicate type (wt. %)	(A)	(B)	(C)
monomer	4.60 \pm 1.4	0.88 \pm 1.2	0.30 \pm 0.8
dimer	1.18 \pm 1.0	0.88 \pm 1.0	1.12 \pm 0.7
3R	0.58 \pm 0.4	0.69 \pm 0.7	0.51 \pm 0.3
4R	1.05 \pm 0.8	0.49 \pm 0.4	0.51 \pm 0.4
D3R	2.00 \pm 1.8	1.71 \pm 1.5	1.68 \pm 1.6
D4R&D5R	4.44 \pm 2.4	1.56 \pm 0.8	0.97 \pm 1.2
Total _{olig}	13.85	6.21	5.09

3R = cyclic trimers, 4R = cyclic tetramers, 3DR = double three rings, D4R = double four rings and D5R = double five rings. Total_{olig} = total amount (wt. %) of Si in the form of monomers and oligomers.

The probable reason for such partial aggregation is that, after the removal of some TPA⁺ ions from the nanoparticle's shell, a part of the monomers and oligomers from the liquid phase

reacts with the exposed terminal silanol groups by forming new $\equiv\text{Si}-\text{O}-\text{Si}\equiv$ linkages. However, since the amount of the partly aggregated monomers and oligomers represents only a few percents of the total Si in the system, this transformation does not influence the size of the PNPs.

The data presented in Table S3 are consistent with the results of the previous investigations^{15,16,21,30,46,49,52} and, at the same time, show that the subsequent addition of NaOH does not considerably affect the distribution of Si–O–Si connectivity (Q^n values). These results are expected since the data in Table S3 is to a greater extent relevant to the nanoparticle core,^{15,16,21,30,46,49,52} and the nanoparticles were formed before addition of NaOH.

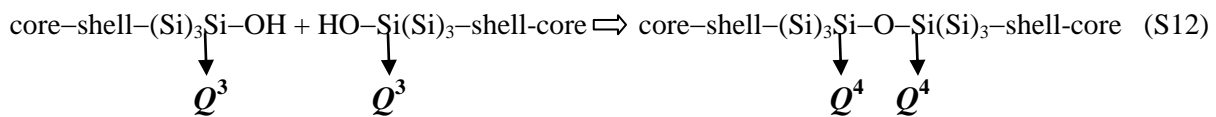
Table S3 The distributions of S–O–Si connectivity (expressed as Q^n , where n is number of bridging oxygen atoms per SiO_4) in the nanoparticles existing in HmRM₀-I (A) and in 1aS-HmRMs, characterized by: $x_s = 0.0036$ (B) and $x_s = 0.0144$ (C). The values of Q^n are taken from the corresponding peak integrals in the ²⁹Si-NMR spectra (see Experimental in the main text). The ²⁹Si-NMR spectra of all the samples are made 24 h hours after preparation ($t_A = 24$ h for $x_s = x_d = 0$) or after subsequent addition of NaOH ($t_A = 24$ h for $x_s = 0.0036$ and $x_s = 0.0144$, respectively; see Experimental in the main text). $Q^{n\Delta}$ corresponds to Si sites with n connectivity present in 3-membered rings. Total_{NP} = total amount (wt. %) of Si in nanoparticles.

HmRM: $\text{SiO}_2:x_s\text{NaOH}(0.36 - x_s)\text{TPAOH:4EtOH:18H}_2\text{O}$			
Q^n (wt. %)	(A)	(B)	(C)
$Q^1 + Q^{2\Delta}$	5.50 \pm 1.2	5.56 \pm 0.8	6.30 \pm 1.4
$Q^2 + Q^{3\Delta}$	10.12 \pm 3.4	13.55 \pm 4.6	13.84 \pm 2.8
Q^3	42.53 \pm 3.0	40.44 \pm 4.2	39.08 \pm 3.5
Q^4	28.00 \pm 2.7	34.24 \pm 1.8	35.69 \pm 4.3
Total _{NP}	86.15	93.79	94.91

However, a slight decrease of the Q^3 sites and simultaneous increase of the Q^4 sites with the increase of x_s , from 0 (A), through 0.0036 (B) to 0.0144 (C), could be influenced by the

changes in the nanoparticles shells during the aggregation processes, initiated by the presence of Na^+ ions.

Since the most of the terminal Si atoms in the nanoparticle shell are $\text{Si}-Q^3$ [core@shell- $(\text{Si})_3\text{Si}-\text{OH}$ and core@shell- $(\text{Si})_3\text{Si}-\text{O}^-$; see Scheme 2 in the main text and Scheme S1 in the SI-3], the formation of the $\equiv\text{Si}-\text{O}-\text{Si}\equiv$ bridges between the shells of the collided nanoparticles (marked by red ellipse in Scheme 2 in the main text), results in the „transformation“ of the reacting terminal $\text{Si}-Q^3$ silicon atoms into $\text{Si}-Q^4$ silicon atoms, i.e.,



On the other hand, since the small differences in the percentages of $\text{Si}-Q^3$ and $\text{Si}-Q^4$ for the investigated HmRMs ($x_s = 0$, $x_s = 0.0036$ and $x_s = 0.0144$; see Table 2), lie in the range of expected errors (see Table S3), the observed decrease of the Q^3 sites and simultaneous increase of the Q^4 sites may be only a coincidence. Therefore, the relationship between the processes in nanoparticles shells and the changes of the Q^3 and Q^4 sites, as expressed by Eq. (S12), cannot be positively proved at present.

Results of the quantitative analysis of the ^{29}Si -NMR spectra of the selected 2D-HmRMs, prepared by direct addition of NaOH (see Experimental in the main text), are shown in Tables 3 and 4. The fraction, x_d , of the directly added NaOH significantly influence neither the distribution of oligomers in solution (Table S4) nor the distribution of Si–O–Si connectivity in nanoparticles (Table S5). The distribution of oligomers in the 2D-HmRMs (Table S4) are comparable with the distribution of oligomers in the 1aS-HmRM, obtained by subsequent addition of NaOH (Table S2) and thus, consistent with the results of previous investigations.^{15,16,21,30,46,49,52} On the other hand, the comparison of Tables S3 and S5 shows that the percentage of Q^4 sites in the 1aS-HmRMs is somewhat higher than the percentage of Q^4 sites in the 2D-HmRMs. One of reasonable explanation could be that the presence of Na^+ ions in the nanoparticle core (see Scheme 3 and corresponding discussion in the main text; also see the corresponding consideration in SI-2) prevents the formation of $\equiv\text{Si}-\text{O}-\text{Si}\equiv$ linkages between the Si atoms with the connectivity $Q^{(n<4)}$.

Table S4 The distribution of Si, in the forms of silicate monomers and polysilicate anions (oligomers), in the 2D-HmRMs, characterized by: $x_d = 0.027$ and $R_d = 0.075$ (A), $x_d = 0.036$, and $R_d = 0.1$ (B) and $x_d = 0.0468$ and $R_d = 0.13$ (C). The weight percentage of Si, in the form of silicate monomers and different polysilicate anions (oligomers), is taken from the corresponding integrals in the ^{29}Si -NMR spectra (see Experimental in the main text) The ^{29}Si -NMR spectra of all the samples are made 24 h hours after preparation ($t_A = 24$ h) by direct addition of NaOH (see Experimental in the main text).

HmRM: $\text{SiO}_2:x_d\text{NaOH}(0.36 - x_d)\text{TPAOH:4EtOH:18H}_2\text{O}$			
(poly)silicate type (wt. %)	(A)	(B)	(C)
monomer	0.39 \pm 0.42	0.38 \pm 0.36	0.37 \pm 0.40
dimer	1.23 \pm 0.56	1.18 \pm 0.62	1.18 \pm 0.42
3R	0.42 \pm 0.33	0.20 \pm 0.22	0.20 \pm 0.18
4R	0.65 \pm 0.40	0.63 \pm 0.54	0.64 \pm 0.36
D3R	2.57 \pm 0.92	2.46 \pm 1.30	2.47 \pm 0.86
D4R&D5R	0.81 \pm 0.63	1.21 \pm 0.80	1.22 \pm 1.0
Total _{olig}	6.07	6.06	6.08

3R = cyclic trimers, 4R = cyclic tetramers, 3DR = double three rings, D4R = double four rings and D5R = double five rings. Total_{olig} = total amount (wt. %) of Si in the form of monomers and oligomers.

Table S6 shows the distributions of Si species, in the form of silicate monomers and polysilicate anions (oligomers) in the NaOH-free HmRM₀-II and in the NaOH-containing 1bS-HmRM, both prepared below the CAC, as it is described in Experimental in the main text. The effect of the partial incorporation of oligomers into the nanoparticles, caused by subsequent addition of NaOH to the NaOH-free 1a-HmRM (see Table S2), was not observed when NaOH was subsequently added to the NaOH-free 1b-HmRM (see Table S6). The obvious reason is that the amount of Si, present in the nanoparticles formed below the CAC, represents only a very small part of the total amount of Si in HmRMs.⁵² Hence, taking into account the experimental errors (see Table S6), eventual partial incorporation of oligomers into nanoparticles could not be detected by the applied method (see Experimental in the main text). By the same reason, the addition of a small amount of NaOH into NaOH-free 1b-HmRM does not considerably change the distribution of monomers and oligomers (see Table S6).

Table S5 The distributions of Si–O–Si connectivity (expressed as Q^n , where n is number of bridging oxygen atoms per SiO_4) in the nanoparticles existing in the 2D-HmRMs, characterized by: $x_d = 0.027$ and $R_d = 0.075$ (A), $x_d = 0.036$ and $R_d = 0.1$ (B), and $x_d = 0.0468$ and $R_d = 0.13$ (C). The values of Q^n are taken from the corresponding peak integrals in the ^{29}Si -NMR spectra (see Experimental in the main text). The ^{29}Si -NMR spectra of all the samples are made 24 h hours after preparation ($t_A = 24$ h) by direct addition of NaOH (see Experimental in the main text). Here, $Q^{n\Delta}$ corresponds to Si sites with n connectivity present in 3-membered rings. Total_{NP} = total amount (wt. %) of Si in nanoparticles.

HmRM: $\text{SiO}_2:x_d\text{NaOH}(0.36 - x_d)\text{TPAOH:4EtOH:18H}_2\text{O}$			
Q^n (wt. %)	(A)	(B)	(C)
$Q^1 + Q^{2\Delta}$	4.35 \pm 0.92	5.23 \pm 1.03	5.06 \pm 0.86
$Q^2 + Q^{3\Delta}$	12.19 \pm 2.60	11.64 \pm 3.43	11.20 \pm 2.80
Q^3	47.82 \pm 3.62	47.02 \pm 4.43	46.80 \pm 3.86
Q^4	14.57 \pm 1.88	14.57 \pm 2.63	14.43 \pm 3.24
Total _{NP}	93.93	93.94	93.92

Table S6 The distributions of Si, in the forms of silicate monomers and polysilicate anions (oligomers), in the HmRM₀-II (A) and in 1bS-HmRM (B), prepared and treated as it is described in Experimental. The weight percentages of Si, in the forms of silicate monomers and different polysilicate anions (oligomers), are provided by the analysis of the corresponding ²⁹Si-NMR spectra (see Experimental in the main text) The ²⁹Si-NMR spectrum of HmRM₀-II was made 24 h after preparation ($t_A = 24$ h; see Experimental in the main text) and the ²⁹Si-NMR spectra of 1bS-HmRM was made 24 h after the addition of NaOH ($t_{A'} = 24$ h; see Methods).

HmRM: 0.2SiO ₂ : x_s NaOH(0.36 – x_s)TPAOH:0.8EtOH:18H ₂ O		
(poly)silicate type (wt. %)	(A) $x_s = 0$	(B) $x_s = 0.0072$
monomer	15.74±1.24	15.67±0.86
dimer	23.83±1.76	22.69±2.05
3R	15.83±1.33	15.18±1.22
4R	31.58±2.40	31.44±2.54
D3R	8.16±0.92	10.18±1.30
D4R&D5R	4.85±0.76	6.83±0.94
Total _{olig}	100.00	100.00

3R = cyclic trimers, 4R = cyclic tetramers, 3DR = double three rings, D4R = double four rings and D5R = double five rings. Total_{olig} = total amount (wt. %) of Si in the form of monomers and oligomers.

Additional references

- A1 A. Beganskiene, V. Sirutkaitis, M. Kurtinairiene, R. Juškenas and A. Kareiva, *Mater. Sci.*, 2004, **10**, 287-290.
- A2 C. J. Brinker, *Non-Crystalline Solids*, 1988, **100**, 31-50.
- A3 M. Castro, M. Haouas, F. Taulelle, I. Lim, E. Breynaert, G. Brabants, C. E. A. Kirschhock and W. Schmidt, *Microporous Mesoporous Mater.*, 2014, **189**, 158-162.
- A4 C. Y. Hsu, A. S. T. Chiang, R. Selvin and R. W. Thompson, *J. Phys. Chem.*, 2005, **109**, 18804-18814.
- A5 G. Brabants, M. Hubin, E. K. Reichel, B. Jakoby, E. Breynaert, F. Taulelle, J. A. Martens and C. E. A. Kirschhock, *Langmuir*, 2017, **33**, 2581–2589.
- A6 E. A. Persson, B. J. Schoeman, J. Sterte and J.-E. Otterstedt, *Zeolites*, 1994, **14**, 557-567.
- A7 B. J. Schoeman, J. Sterte and J.-E. Otterstedt, *Zeolites*, 1994, **14**, 568-575.

A8 P.-P- E. A. de Moor, T. P. M Beelen and R. A. van Santen, *J. Phys. Chem. B*, 1999, **103**, 1639-1650.

A9 Q. Li, B. Mihailova, D. Creaser and J. Sterte, *Microporous Mesoporous Mater.*, 2001, **43**, 51-59.

A10 E. G. Derouane, S. Detremmerie, Z. Gabelica and N. Blom, *Appl. Catal.*, 1981, **1**, 201-224.

A11 Z. Gabelica, N. Blom and E. G. Derouane, *Appl. Catal.*, 1983, **5**, 227-248.

A12 M. Salou, F. Kooli, Y. Kiyozumi and F. Mikamizi, *J. Mater. Chem.*, 2001, **11**, 1476-1481.